European Polymer Journal 232 (2025) 113929

Contents lists available at ScienceDirect

European Polymer Journal

journal homepage: www.elsevier.com/locate/europolj

Overcoming synthetic challenges in developing High-Performance polybenzoxazine from Diamine-Functionalized Double-Decker silsesquioxane (DDSQ) cage

Hui-Wen Chen, Mohamed Gamal Mohamed, Yang-Chin Kao, Wei-Cheng Chen, Kevin Chiou, Shiao-Wei Kuo *

Department of Materials and Optoelectronic Science, Center for Functional Polymers and Supramolecular Materials, National Sun Yat-Sen University, Kaohsiung 80424, Taiwan

ARTICLE INFO

Keywords:
Diamine-DDSQ
Benzoxazine
Schiff-base Reaction
Thermal Property
Microporous Materials

ABSTRACT

A new diamine-functionalized double-decker silsesquioxane (DDSQ-NH_2) derivative was first synthesized from the phenyltrimethoxysilane as the starting material by following sol–gel reaction in NaOH to form DDNa, corner capping with methylvinyldichlorosilane to form the DDSQ-CH=CH_2 derivative and finally reacted with 4-bromoaniline by using Heck reaction to obtain the target compound. Various synthetic approaches, including one-pot Mannich condensation and three-step synthesis based on this new diamine-functionalized DDSQ (DDSQ-NH_2) compound, were explored but proved unsuccessful due to low selectivity and DDSQ structural degradation. The novel DDSQ-based benzoxazine monomer (DDSQ-BZ (III) in this study) was successfully synthesized through a Schiff-base reaction between DDSQ-NH_2 and 3-phenyl-3,4-dihydro-2H-benzo[e][1,3]oxazine-6-carbaldehyde (CHO-BZ) monomer, maintaining the fully closed-cage DDSQ structure, which is thoroughly characterized using FTIR, NMR, DSC, and TGA analyses, confirming the retention of the DDSQ cage and the formation of the benzoxazine ring. Thermal polymerization behavior was analyzed, revealing record-high stability (T_{d10} = 644 °C, char yield = 82.8 wt%). TEM, SEM, and EDX analyses demonstrated homogeneous dispersion of the DDSQ cage structure within the polybenzoxazine matrix, ensuring enhanced thermal stability.

1. Introduction

Organic polymeric materials are essential in various electronic automotive and aerospace applications [1–3]. Among these, benzoxazine (BZ) resins have received much attention because of their high heat resistance, flexible molecular design, stable dimensional and dielectric constant, and low surface free energy compared with the traditional phenolic or epoxy resin [4–13], which have potential applications in surface coatings [14–17], adhesives [18] and nanocomposites [19–21]. The synthesis of benzoxazine derivatives typically involves the Mannich condensation of primary aromatic or aliphatic amines, phenolic derivatives, and CH_2O in various solvents. During thermal ring-opening polymerization (ROP), the benzoxazine monomer could form a highly three-dimensional (3D) crosslinked polymer network without any byproducts releasing [22–25].

Despite their excellent properties, the typical benzoxazine resins also meet some limitations in terms of thermal stability and chemical resistance at relatively higher temperature environments (for example > 250 °C for silicon carbide (SiC) device packing) [26]. To overcome these challenges, there has been significant interest in modifying the chemical structures of benzoxazine resin to improve their physical properties in extreme conditions. Using inorganic nanoparticles to form organic/inorganic polybenzoxazine hybrids is the typical approach to enhance their thermal performance [27,28] carbon-based nanoparticles including carbon black, carbon nanotube, or graphene [29–33]; however, carbon-based nanoparticles often lack covalent bonding with the polybenzoxazine matrix, limiting their effectiveness [34–36]. As a result, silicon-based such as polydimethylsiloxane (PDMS), nanoclay silicate, or polyhedral oligomeric silsesquioxane (POSS) have been widely used in the polybenzoxazine matrix [37–43]. Among these, the most efficient approach for synthesizing polybenzoxazine/POSS nanocomposites involves establishing covalent linkages within the polymer/POSS hybrid structure [44–46]. Therefore, incorporating a POSS silica cage into the polymer network can improve their characteristics such as

* Corresponding author.
E-mail address: kuosw@faculty.nsysu.edu.tw (S.-W. Kuo).

https://doi.org/10.1016/j.eurpolymj.2025.113929
Received 5 March 2025; Received in revised form 21 March 2025; Accepted 5 April 2025
Available online 6 April 2025

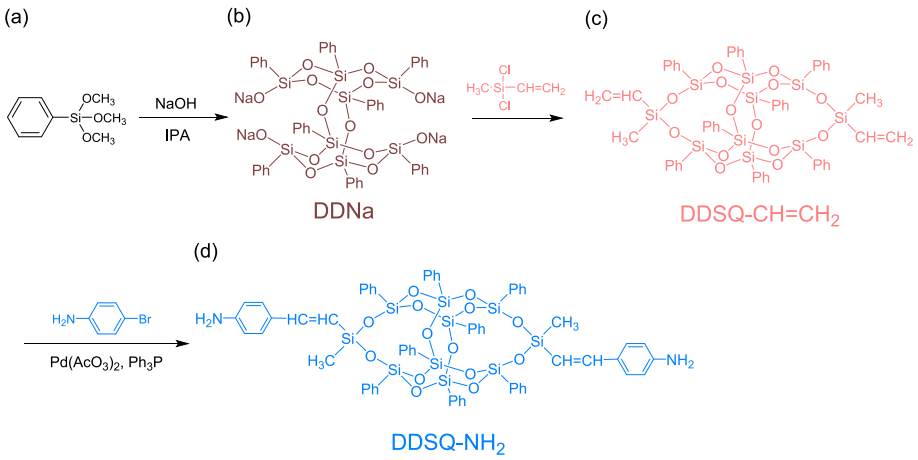

Scheme 1. The preparation of diamine-functionalized DDSQ cage (DDSQ-NH_2) (d) from (a) phenyltrimethoxylsilane, (b) DDNa, and (c) DDSQ-CH=CH_2 compounds.

high-temperature stability, dimensional stability, and flame retardancy [47–52].

In our previous studies [53–55], we presented a comprehensive analysis of the diverse structural configurations of polymer/POSS hybrid systems, which are largely dependent on the functionalization of POSS derivatives. For polybenzoxazine/POSS hybrids, many previous studies have used mono- or octa-functionalized POSS monomers to form their corresponding nanocomposites [44,56–58]. Another strategy for developing polybenzoxazine/POSS hybrids involves incorporating di-functionalized POSS nanoparticles and thus the DDSQ into the BZ resins has also been investigated [59–62]. DDSQ is a class of organic/inorganic hybrid compounds that combine heat resistance and structural rigidity with the reactivity and versatility of organic functional groups. These unique behaviors make it an ideal candidate for improving the thermal and chemical stability of polymer/DDSQ hybrids of the main-chain type, such as polyimide [63–65], polyurethane [66–68], block copolymer [69–71], and polybenzoxazine [59–62] systems.

In our previous studies [72–75], the polybenzoxazine/DDSQ hybrids were all synthesized from the functionalized phenolic DDSQ derivatives, and thus the DDSQ-BZ monomer could be easily synthesized by one-pot Mannich condensation with primary amine (such as aniline and allyl amine) and CH_2O. However, even though these DDSQ-BZ monomers already exhibited very high-temperature stability [up to the 10 % weight loss temperature (T_{d10}) = 521 °C and char yield = 75.0 wt%] [73], some attempts have been used DDSQ cage into the BZ monomer to improve their physical properties further. In particular, the studies on the synthesis of diamine-functionalized DDSQ derivatives have shown that these monomers could provide a versatile platform for developing new polybenzoxazine resins. However, it did not consistently enable the successful synthesis of benzoxazine resin due to the low selectivity, especially in diamine monomers [76–78]. Lin and Ishida et al. proposed another approach for the preparation of benzoxazine monomers by using three-step methods involving forming a Schiff base with 4-hydroxybenzaldehyde, followed by reduction using $NaBH_4$, and the ring-closing Mannich condensation with CH_2O and then affords the benzoxazine monomer without any side reaction [76–78]. This three-step method became the typical approach to synthesizing the oxazine ring for multifunctional amine monomers in our previous studies [79–83]. However, the POSS cage structure is an easy partially hydrolyzed open cage structure with $NaBH_4$ reduction agent [84], which would break the Si-O-Si bonds in POSS under certain conditions. To maintain the fully closed condensed cage DDSQ structure and the oxazine ring in DDSQ-BZ monomer, the reaction condition required to synthesize based on diamine DDSQ monomer (DDSQ-NH_2) is often challenging, involving multi-step processes with potential side reactions that must be mediated to achieve the desired physical properties.

In light of these challenges, this study aims to address the synthesis difficulties associated with the DDSQ-BZ monomer by exploring new synthetic routes with fewer steps. As a result, a new DDSQ-NH_2 derivative was first synthesized in this study. Various synthetic approaches, including one-pot Mannich condensation and three-step synthesis based on this new DDSQ-NH_2 compound, were explored but proved unsuccessful due to low selectivity and DDSQ structural degradation. As a result, the novel DDSQ-based benzoxazine monomer (DDSQ-BZ) in this study was successfully synthesized through a Schiff-base reaction between DDSQ-NH_2 and CHO-BZ monomer directly, maintaining the fully closed-cage DDSQ structure and the formation of the benzoxazine ring. The record-high thermal stability of the benzoxazine resin from diamine-functionalized DDSQ cage structure after thermal ROP procedures was obtained (up to T_{d10} = 644 °C and char yield = 82.8 wt%) and thus this work highlights the significant role and synthesis challenges of benzoxazine monomer based on diamine-functionalized DDSQ, making it a promising candidate for next-generation high-temperature materials.

2. Experimental Section

2.1. Materials

Phenyltrimethoxysilane (97 %), sodium hydroxide, triphenylphosphine (98 %), phenol (99 %), aniline, salicylaldehyde (99 %), and sodium borohydride were purchased from Sigma-Aldrich. Toluene, tetrahydrofuran (THF), triethylamine, methanol, isopropanol, 1,4-dioxane, and ethanol were purchased from Merck and were dried over CaH_2 for 24 h. Methylvinyldichlorosilane (97 %), 4-bromoaniline (99 %), palladium(II) acetate, paraformaldehyde, and 4-hydroxybenzaldehyde were purchased from Alfa-Aesar. In our prior research, the synthesis of DDSQ and DDNa was successfully achieved, as depicted in Scheme 1**(b)** [69,72–74].

2.2. Synthesis of vinyl Double-Decker silsesquioxane (DDSQ-CH=CH_2)

Methylvinyldichlorosilane (4.50 g, 20.0 mmol), DD-Na (11.60 g, 5.00 mmol), triethylamine (4.00 g), and THF (150 mL) were put into the flask equipped with the ice bath and stirred for 6 h. The solution was further stirred at room temperature for 6 h. The filtrate was washed with deionized water, extracted with DCM, and dried over $MgSO_4$. Through vacuum distillation, the DCM solution was concentrated and then dried in a vacuum oven to give the white solids (yield: 70 %). FTIR (KBr, cm^{-1}): 1605 (Si-CH=CH_2), 1260 (Si-CH_3), 1132 (Si-O-Si). ^{1}H NMR (500 MHz, $CHCl_3$-*d*, δ, ppm): 7.56–7.17 (Ar-**H**), 6.20 and 5.92 (Si-CH=CH_2), 0.37 (Si-CH_3).

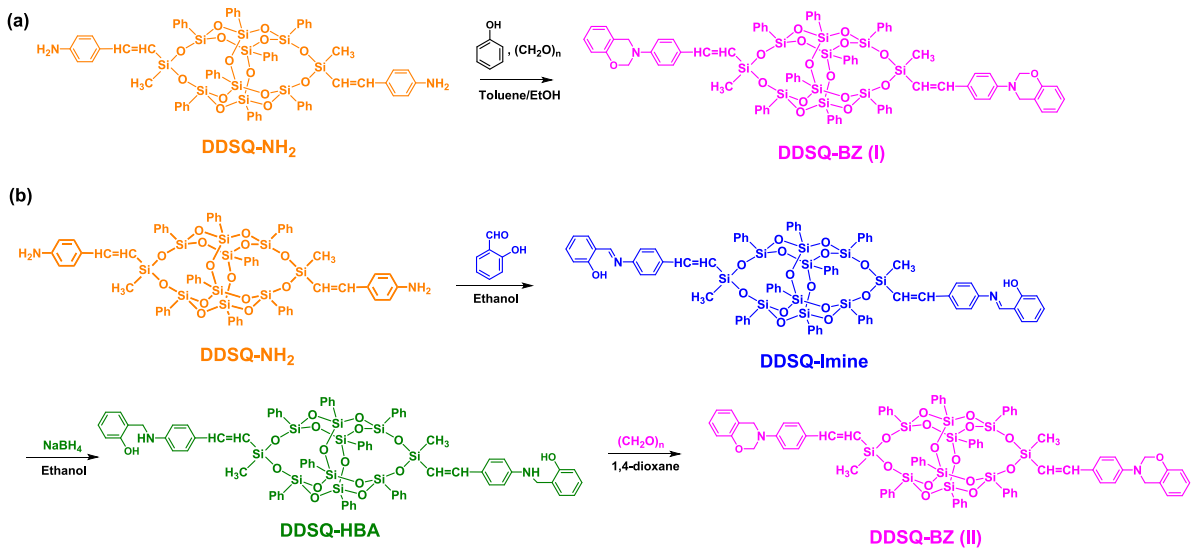

Scheme 2. (a) The synthesis of DDSQ-BZ (I) monomer from DDSQ-NH_2 by using one-pot Mannich condensation and (b) the synthesis of DDSQ-BZ (II) monomer from DDSQ-NH_2 by using a three-step approach.

2.3. *Synthesis of Dianilino Double-Decker silsesquioxane (DDSQ-NH_2)*

Under N_2, DDSQ-CH=CH_2 (6.05 g, 10 mmol), 4-bromoaniline (8.10 g, 100 mmol), $Pd(OAc)_2$ (125 mg), and triphenylphosphine (270 mg) were placed in a flask with 150 mL of anhydrous toluene and triethylamine (20 mL) and kept refluxed at 100 °C for 72 h. The resulting mixture was filtered and concentrated through rotary evaporation. After dropping the mixture solution into methanol, the precipitate was vacuum-dried at 30 °C for 24 h to obtain a powder. FTIR (KBr, cm^{-1}): 3466 and 3402 (NH_2 group), 1132 (Si-O-Si). ^1H NMR (500 MHz, $CHCl_3$-*d*, δ, ppm): 7.07–6.92 (CH=CH-Ph), 6.20 and 5.92 (Si-CH=CH), 3.72 (NH_2).

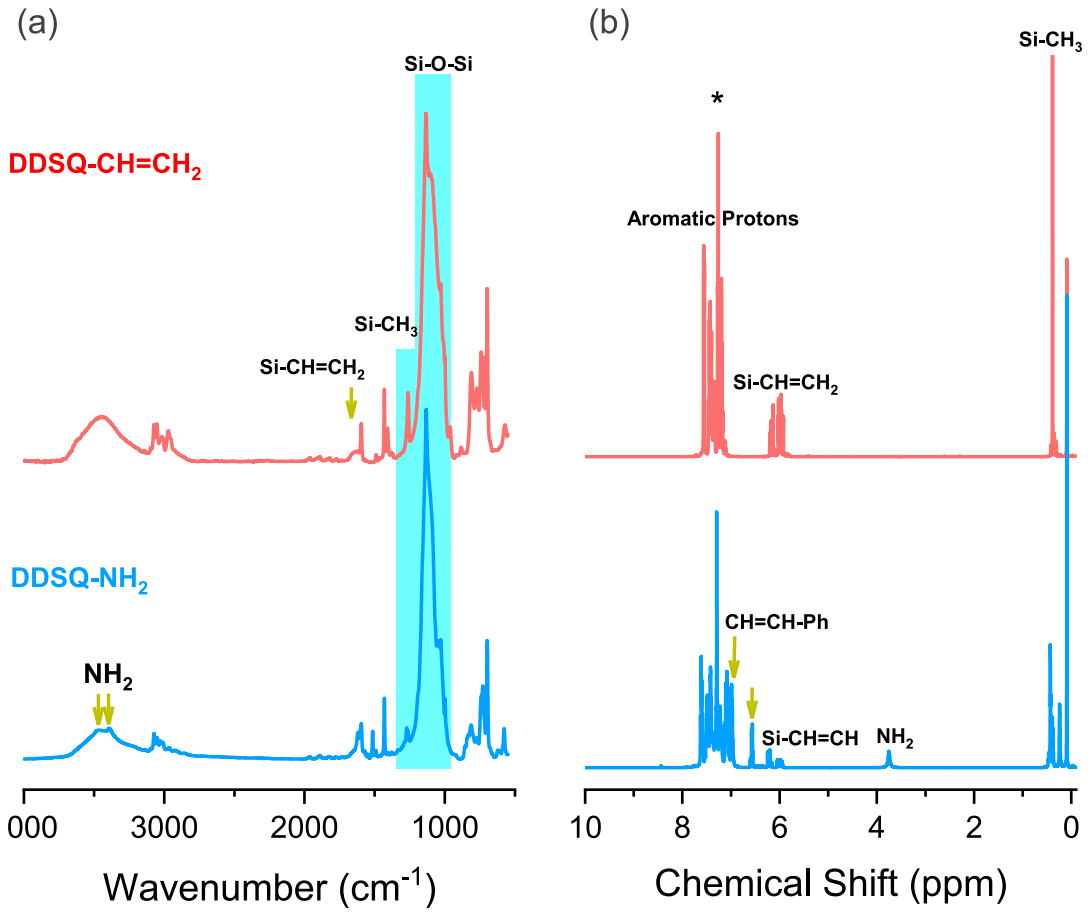

Fig. 1. (a) FTIR and (b) ^1H NMR spectra of DDSQ-CH=CH_2 and DDSQ-NH_2 derivatives.

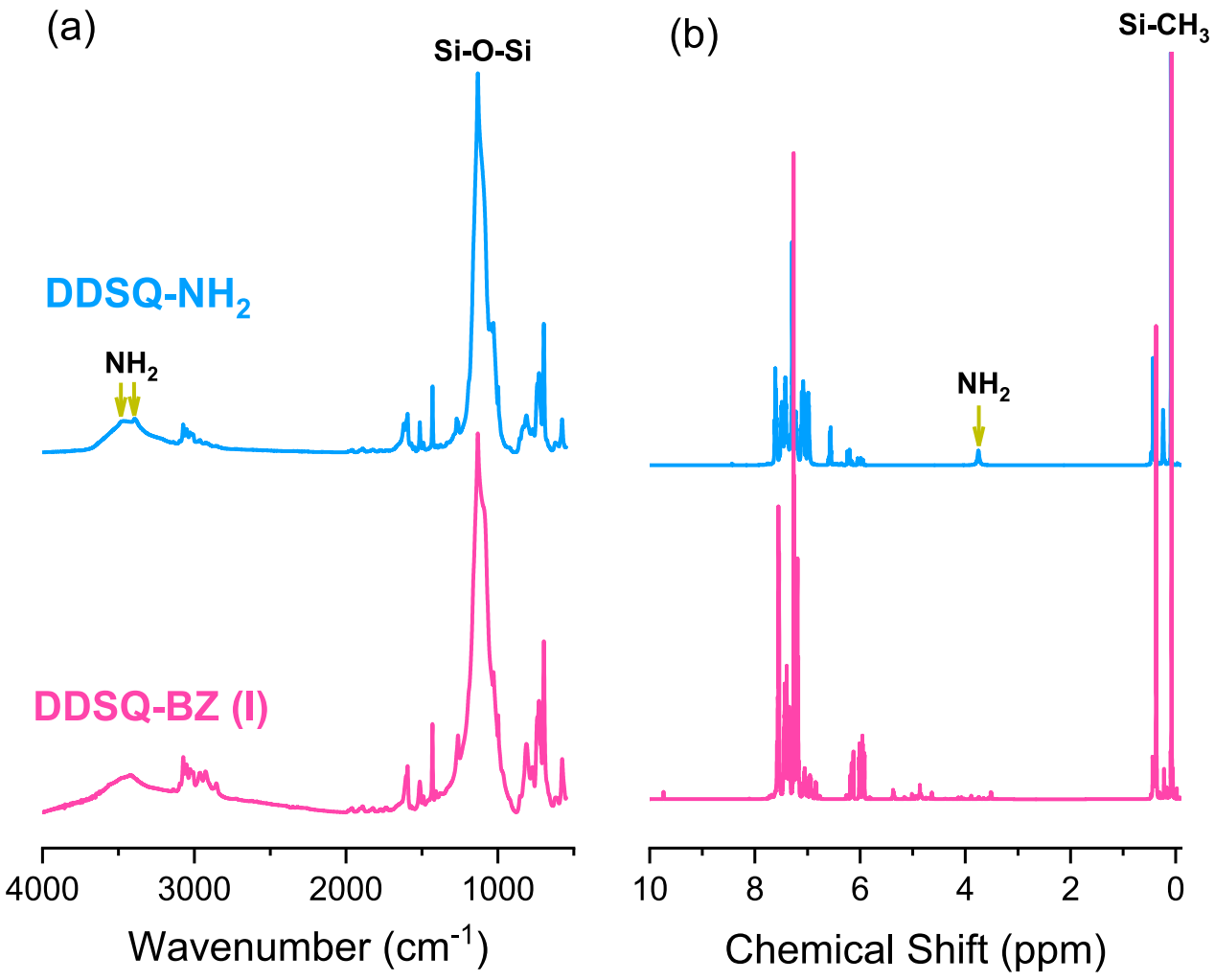

Fig. 2. (a) FTIR and (b) ^{1}H NMR spectra of DDSQ-NH_2 and DDSQ-BZ (I) monomer.

2.4. *One-Pot Mannich condensation of DDSQ-BZ (I) from DDSQ-NH_2 monomer*

DDSQ-NH_2 (1.0 g, 0.72 mmol), phenol (0.142 g, 1.51 mmol), and paraformaldehyde (0.092 g, 3.03 mmol) reacted in a solvent mixture of toluene/ethanol (75 mL, ratio = 2/1) at 100 °C for 48 hr. The solution was extracted with 1 N sodium hydroxide and dried with anhydrous $MgSO_4$. After filtering, the solvent was removed by a rotary evaporator and then the yellow solid was obtained (yield: 78 %), as presented in Scheme 2**(a)**. FTIR (KBr, cm^{-1}): 3067 (CH aromatic), 1132 (Si-O-Si). ^{1}H NMR (500 MHz, $CHCl_3$-*d*, δ, ppm): 4.86 (triazine ring).

2.5. *Three-Step synthesis of DDSQ-BZ (II) from DDSQ-NH_2 monomer*

Salicylaldehyde (0.188 mL, 1.8 mmol), ethanol (75 mL), and DDSQ-NH_2 (0.5 g, 0.36 mmol) were added to a round flask and refluxed at 75 °C for 24 h. The resulting yellow solid, DDSQ-Imine, was filtered, washed with ethanol, and dried. $NaBH_4$ (0.285 g), DDSQ-Imine (1.0 g, 0.63 mmol), and DMAc (20 mL) reacted for 24 h at 25 °C. After pouring into 1 L of water and filtering, the precipitates DDSQ-HBA were obtained. The synthesis of DDSQ-BZ(II) was synthesized from a mixture of DDSQ-HBA (0.8 g, 0.5 mmol), 1,4-dioxane (50 mL), paraformaldehyde (0.07 g, 2.33 mmol), and ethanol (25 mL) were stirred at 90 °C for 24 hr. The blend was washed with 1 N sodium hydroxide solution three times and then removed the solvent via vacuum distillation. After drying, the yellow powder was obtained (yield: 82 %). FTIR (KBr, cm^{-1}): 1132 (Si-O-Si), 946 (oxazine ring). ^{1}H NMR (500 MHz, $CHCl_3$-*d*, δ, ppm): 5.37 (OCH_2N), 4.63 ($ArCH_2N$).

2.6. *Synthesis of 3-phenyl-3,4-dihydro-2H-benzo[e][1,3]oxazine-6-carbaldehyde (CHO-BZ) monomer*

Aniline (2.0 g, 0.02 mol) and paraformaldehyde (1.29 g, 0.04 mol) were dissolved in toluene at 80 °C for 2 hr in a round-bottom flask. Then, *p*-hydroxybenzaldehyde (2.62 g, 0.02 mol) was added and the system was refluxed for another 5 hr. The resulting solution was extracted with 1 N sodium hydroxide and dried over anhydrous $MgSO_4$. The organic layer was recrystallized from toluene to obtain a white crystal powder (yield: 88 %). FTIR (KBr, cm^{-1}): 2845 and 2745 (H-C=O), 1682 (C=O), 948 (oxazine ring). ^{1}H NMR (500 MHz, $CHCl_3$-*d*, δ, ppm): 9.83 (H-C=O), 5.45 (OCH_2N), 4.69 ($ArCH_2N$).

2.7. *Synthesis of DDSQ-BZ (III) monomer from DDSQ-NH_2 and CHO-BZ by Schiff-base reaction*

Ethanol (20 mL), DDSQ-NH_2 (0.5 g, 0.36 mmol), and CHO-BZ (0.22 g, 0.92 mmol) were refluxed at 75 °C for 24 h. The product was filtered, washed with ethanol, and dried, yielding a yellow solid (yield: 91 %). FTIR (KBr, cm^{-1}): 3089, 1270, 1136, 961 (oxazine ring). ^{1}H NMR (500 MHz, $CHCl_3$-*d*, δ, ppm): 8.32 (H-C=N), 5.45 (OCH_2N), 4.68 ($ArCH_2N$).

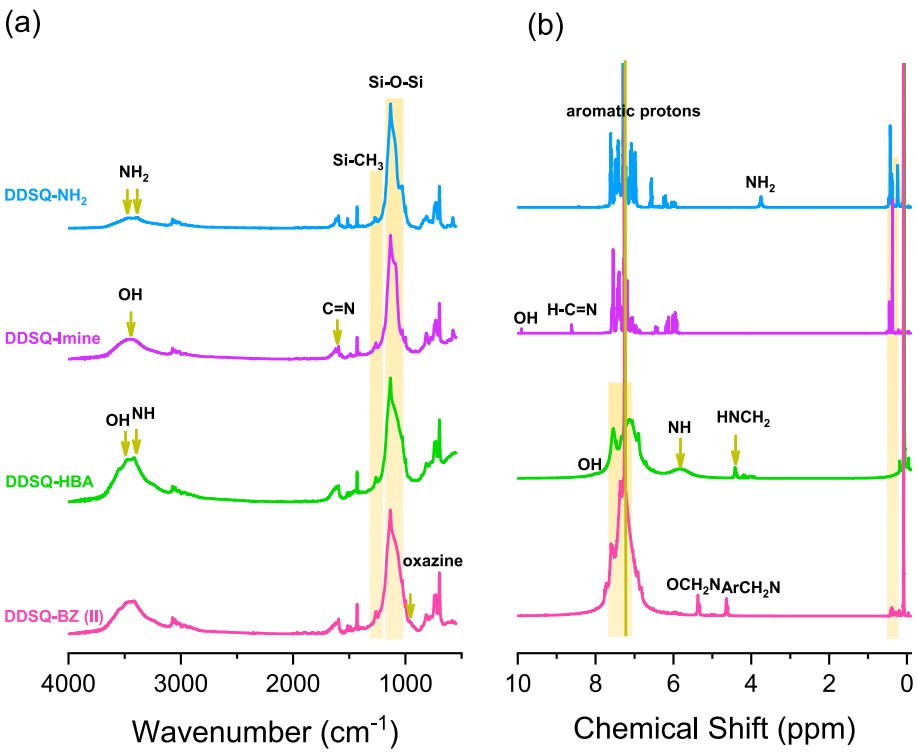

Fig. 3. (a) FTIR and (b) ^{1}H NMR spectra of DDSQ-NH_2, DDSQ-Imine, DDSQ-HBA, and DDSQ-BZ (II) monomers.

2.8. *Thermal polymerization* ***of DDSQ-BZ (III) monomers***

DDSQ-BZ (III) monomers placed in an aluminum pan were heated in steps at the specified temperatures for 2 h each 150, 180, 210, 240, and 270 °C in a vacuum oven to obtain DDSQ-PBZ a dark red color.

3. Results and Discussion

3.1. ***Synthesis of DDSQ-NH_2 diamine*** *monomer*

The synthesis of DDSQ-NH_2 was summarized in Scheme 1 from phenyltrimethoxysilane as a starting material, then prepared the double-decker silsesquioxane-Na (DD-Na) by sol–gel reaction in a basic medium and finally use corner capping method with ethylenedichlorosilane to form the DDSQ-CH=CH_2 monomer. The DDSQ-NH_2 was obtained from DDSQ-CH=CH_2 with 4-bromoaniline by using the Heck reaction. The corresponding chemical structures of DDSQ-CH=CH_2 and DDSQ-NH_2 were identified by using FTIR and ^{1}H NMR spectroscopy as displayed in Fig. 1. For example, Fig. 1**(a)** shows the FTIR spectra of DDSQ-CH=CH_2 and DDSQ-NH_2, where a strong absorption at ca. 1132 cm^{-1} was due to the Si-O-Si unit and the Si-CH_3 group was located at 1260 cm^{-1}, which are typical features for the absorption of DDSQ derivatives [72–74]. Furthermore, the Si-CH=CH_2 double bond signal had appeared at 1605 cm^{-1} for pure DDSQ-CH=CH_2 monomer. Notably, the signals at 3466 and 3395 cm^{-1}, characteristic of DDSQ-NH_2, appeared after heck reaction with 4-bromoaniline, corresponding to asymmetric and symmetric NH absorption, respectively, indicating the effective synthesis of DDSQ-NH_2. Additionally, Fig. 1**(b)** presents the ^{1}H NMR spectra of DDSQ-CH=CH_2 and DDSQ-NH_2, showing the Si-CH_3 signal at 0.37 ppm, and the aromatic protons were found at 7.56–7.17 ppm for both DDSQ compounds. The signal of Si-CH=CH_2 units of DDSQ-CH=CH_2 monomers was found at 6.20 and 5.92 ppm and the integral ratio was 1:2 as expected. After the Heck reaction, the ratio was changed to 1:1 as expected and the aromatic ring from 4-bromoaniline was observed at 7.07 and 6.92 ppm. Most importantly, the NH_2 group was clearly observed at 3.72 ppm, also suggesting the successful formation of the DDSQ-NH_2.

3.2. *Synthesis of DDSQ-BZ (I) from DDSQ-NH_2 monomer by One-Pot Mannich condensation*

The one-pot Mannich condensation is the common and efficient approach for the preparation of benzoxazine from aromatic phenol, paraformaldehyde, and aliphatic/aromatic amine in a single step, leading to the formation of the benzoxazine ring. However, it did not consistently enable successful synthesis of benzoxazine resin due to the low selectivity, especially in diamine monomers. In the first study, we tried to synthesize our DDSQ-BZ (I) monomer through the one-pot Mannich condensation presented in Scheme 2**(a)** from DDSQ-NH_2, phenol, and paraformaldehyde.

Fig. 2 shows their corresponding FTIR and ^{1}H NMR spectroscopy, the NH_2 units in FTIR (Fig. 2**(a)**) and ^{1}H NMR spectra (Fig. 2**(b)**) both disappeared; however, it did not observe the benzoxazine ring absorption or chemical shift and the related triazine unit was found at ca. 4.86 ppm, indicating the synthesis of DDSQ-BZ (I) is not successful by using one-pot Mannich condensation based on our DDSQ-NH_2 in this study.

3.3. ***DDSQ-BZ (II) from DDSQ-NH_2 monomer by Three-Step synthesis***

A three-step synthesis of the benzoxazine monomer from a diamine system was another typical approach by the formation of Schiff-base imine formation, reduction of the Schiff-base imine group, and the Mannich reaction. Scheme 2**(b)** displayed the formation of DDSQ-BZ (II) monomer from the DDSQ-NH_2 with salicylaldehyde to provide DDSQ-Imine by the Schiff base reaction. In the second step, the imine (C=N) group was converted to an NH-CH_2 unit through $NaBH_4$ reduction to prepare the DDSQ-HBA compound. Finally, the DDSQ-BZ (II) monomer was synthesized via.

Mannich condensation with $(CH_2O)_n$ in 1,4-dioxane at 90 °C, which is generally approached to prepare the multifunctional benzoxazine rings based on diamine, tri-amine or tetra-amine systems in our previous studies [78–83]. The FTIR spectrum of the DDSQ-NH_2 [Fig. 3**(a)**] featured signals at 3466 and 3402 cm^{-1} for NH_2 stretching as mentioned

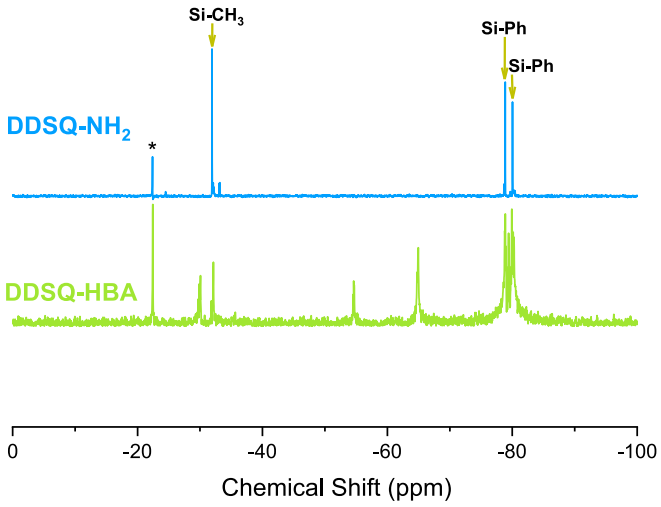

Fig. 4. ^{29}Si NMR spectra of (a) DDSQ-NH_2 and (b) DDSQ-HBA monomer.

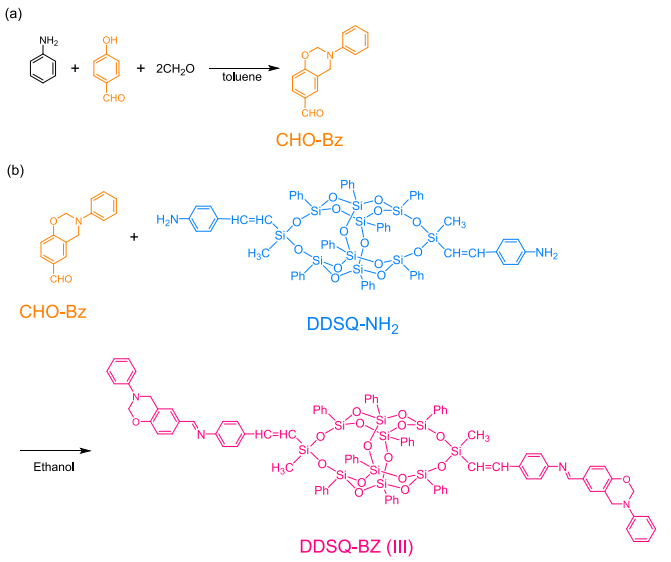

Scheme 3. (a) The synthesis of CHO-BZ monomer by using one-pot Mannich condensation and (b) the synthesis of DDSQ-BZ (III) monomer using DDSQ-NH_2 and CHO-BZ by Schiff-base reaction.

previously and the strong absorption at ca. 1132 cm^{-1} was owing to the Si-O-Si unit and the Si-CH_3 group was located at 1259 cm^{-1}, which were all observed for all DDSQ derivatives in this study. The FTIR spectrum of DDSQ-Imine possesses a broad peak at 3446 cm^{-1} for OH unit and 1625 cm^{-1} for C=N unit. After reduction with $NaBH_4$ to form DDSQ-HBA, the broad absorptions were observed at 3499, and 3415 cm^{-1} owing to the OH and NH groups. Ultimately, following Mannich condensation with $(CH_2O)_n$ to form DDSQ-BZ (II), a very small absorption peak was observed at 946 cm^{-1} due to the oxazine unit.

Fig. 3**(b)** shows the corresponding ^{1}H NMR spectra of each DDSQ compound. The NH_2 group was observed at 3.72 ppm for the DDSQ-NH_2, and this peak almost completely disappeared for DDSQ-Imine and the other signals were present at 9.90 and 8.61 ppm, corresponding to phenolic OH and H-C=N units, respectively. After reduction with $NaBH_4$ to form DDSQ-HBA, the signals at 4.42, 5.81, and 8.00 ppm because of its $HNCH_2$, NH, and OH protons were observed, respectively. The ^{1}H NMR spectrum of the DDSQ-BZ (II) monomer featured the signal at 5.37 ppm (OCH_2N) and 4.63 ppm ($ArCH_2N$), indicating the formation of an oxazine ring. Consequently, we understood that the formation of the oxazine ring of DDSQ-BZ (II) was obtained from the DDSQ-NH_2 by three-step synthesis based on FTIR and NMR spectroscopy analyses. However, we observed that the aromatic protons in Fig. 3**(b)** and the Si-O-Si unit in Fig. 3**(a)** become very broad reductions with $NaBH_4$ to form DDSQ-HBA and DDSQ-BZ (II). Since POSS could exist in a fully closed condensed or partially hydrolyzed open cage structure $NaBH_4$ is commonly used for reducing the C=O unit or breaking Si-O-Si bond in silsesquioxanes under certain conditions [84]. Fig. 4 presents the ^{29}Si NMR spectra of DDSQ-NH_2 and DDSQ-HBA to further confirm the possible open cage structure, in the spectrum of DDSQ-NH_2, the O_2-Si-CH_3(CH=CH_2) resonance appears at −31.84 ppm, while the O_3-Si-Ph signals are detected at −78.87 and −80.01 ppm, indicating the varied surroundings of Si atoms within the DDSQ-NH_2 framework [Fig. 4**(a)**]. Furthermore, Fig. 4**(b)** shows the ^{29}Si NMR spectrum of DDSQ-HBA, there are many new signals observed such as −79.47, −64.97, −54.64, −29.92 ppm, indicating the possible Si-OH and Si-H functional groups may occur, leading to an open-cage POSS structure and it is usually for further functionalization or grafting reaction in polymer/POSS nanocomposites [84].

To confirm the chemical structure of open-cage POSS structure from $NaBH_4$ reduction, we also prepare the 2,2′-((1E,1′E)-((oxybis(4,1-phenylene))bis(azaneylylidene))bis(methaneylylidene)) diphenol (ODA-Imine) and 2,2′-(((oxybis(4,1-phenylene))bis(azanediyl))bis(methylene))diphenol (ODA-HBA) model compound from 4,4-oxydianiline (ODA) as shown in **Scheme S1**. Only the $NaBH_4$ agent could have the reduction reaction where the C=N unit at 1621 cm^{-1} of ODA-Imine was transformed into NH unit at 3260 cm^{-1} of HBA compound by FTIR analyses as shown in **Fig. S1**. In addition, we also used a typical model DDSQ cage structure under reduction with $NaBH_4$, and **Fig. S2** shows their corresponding FTIR spectra recorded at room temperature. The open-cage POSS was also observed since the Si-O-Si unit also became very broad under reduction with $NaBH_4$. Based on FTIR and NMR spectroscopy analyses, we can confirm that the benzoxazine ring was obtained; however, the open-cage POSS structure was observed under reduction with $NaBH_4$ and thus the synthesis of pure DDSQ-BZ (II) is also not successful by three-step pathway based on our DDSQ-NH_2 in this study.

3.4. DDSQ-BZ (III) monomer from DDSQ-NH_2 and CHO-BZ by Schiff-base reaction

To maintain the fully closed condensed DDSQ structure, the $NaBH_4$ reduction could not be used for the synthesis of the DDSQ-BZ (II) compound. Herein, we proposed another pathway to synthesize DDSQ-BZ (III) monomer from DDSQ-NH_2 and CHO-BZ by Schiff-base reaction as shown in Scheme 3. Firstly, we synthesized CHO-BZ monomer from *p*-hydroxybenzaldehyde, aniline, and paraformaldehyde by using Mannich condensation as displayed in Scheme 3**(a)**. Fig. 5**(a)** shows the FTIR spectrum of CHO-BZ monomer where the feature signals for C=O at 1682 cm^{-1}, aldehyde CH at 2745 cm^{-1} and 2845 cm^{-1}, and oxazine ring at 948 cm^{-1} [85,86]. Fig. 5**(b)** shows the corresponding ^{1}H NMR spectrum of CHO-BZ monomer. The peaks corresponding to the aromatic hydrogen atoms appeared at 7.65–6.90 ppm, the CHO proton observed at 9.83 ppm, and the featured signals at 4.69 and 5.45 ppm due to $ArCH_2N$ and OCH_2N units, respectively. The DSC spectrum of the CHO-BZ revealed a melting point at 103 °C and a distinct exothermic polymerization peak at 256 °C with an enthalpy of 391.3 J g^{-1}, as displayed in Fig. 5**(c)**, indicating the high purity of this benzoxazine monomer. Furthermore, the CHO-BZ monomer of TGA analysis (Fig. 5**(d)**) exhibited a T_{d10} of 231 °C close to the thermal ring-opening polymerization (ROP) peak and the char yield of 49.3 wt%. Based on FTIR, NMR, DSC, and TGA analyses, it supports the production of the CHO-BZ. Finally, we constructed the DDSQ-BZ (III) from DDSQ-NH_2 and CHO-BZ by Schiff-base reaction in absolute ethanol at 75 °C for 24 h as shown in Scheme 3**(b)**.

The existence of a fully closed condensed cage DDSQ structure and the oxazine ring in DDSQ-BZ (III) was characterized by using spectroscopy instruments [FTIR and NMR] as shown in Fig. 6. After the Schiff-

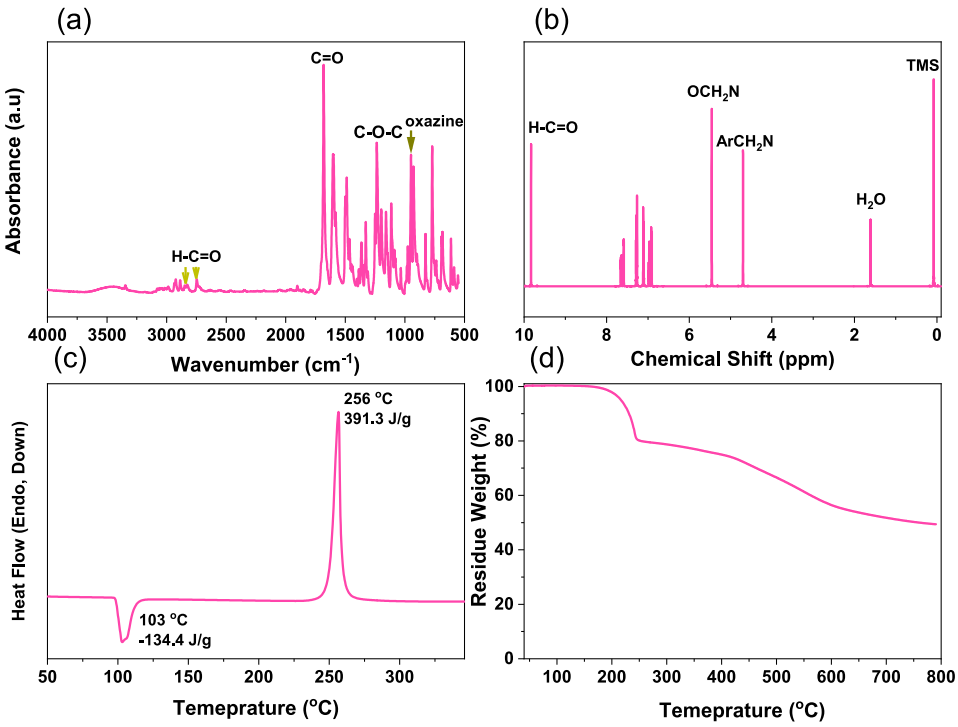

Fig. 5. (a) FTIR, (b) ^{1}H NMR, (c) DSC, and (d) TGA analyses of CHO-BZ monomer.

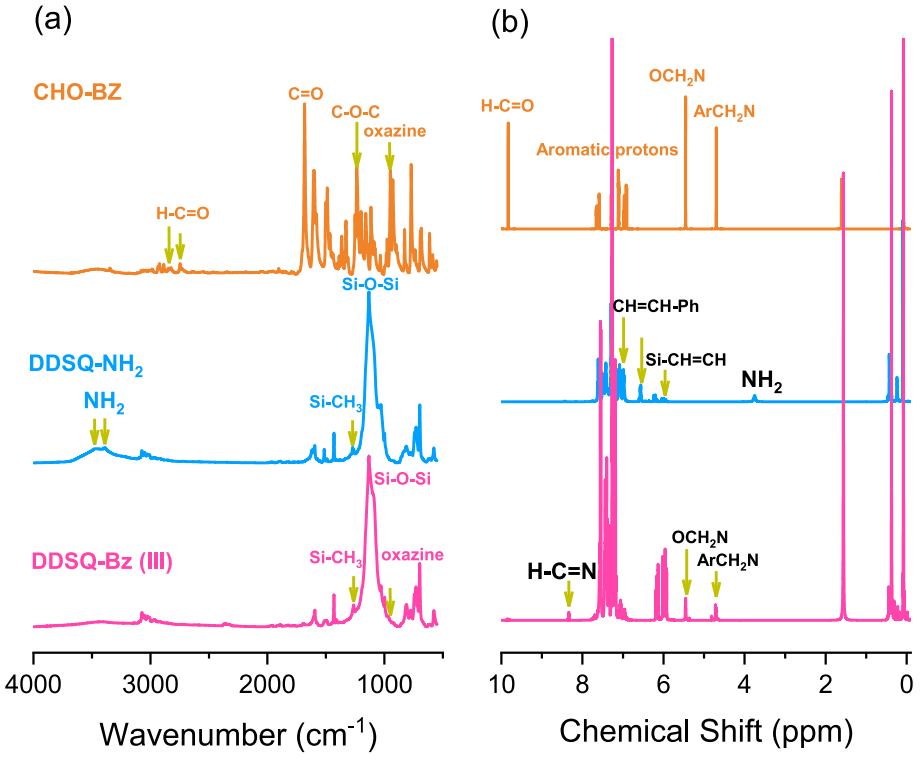

Fig. 6. (a) FTIR and (b) ^{1}H NMR spectra of CHO-BZ, DDSQ-NH_2, and DDSQ-BZ (III) monomer.

base reaction, the disappearance of the aldehyde group (C=O at 1682 cm^{-1} and aldehyde CH at 2745 and 2845 cm^{-1}), along with the appearance of the oxazine ring at 961 cm^{-1}. Most importantly, the Si-O-Si unit at 1136 cm^{-1} had maintained a sharp absorption for DDSQ-BZ (III) monomer by FTIR analyses as shown in Fig. 6**(a)**. This finding was also confirmed by the ^{1}H NMR spectrum of DDSQ-BZ (III) as displayed in Fig. 6**(b)**. The signal for the CHO proton at 9.83 ppm from CHO-BZ was almost completely disappeared and a new imine (H-C=N) bond was observed at 8.31 ppm for the DDSQ-BZ (III) monomer. Furthermore, two distinct signals at 4.68 ppm and 5.45 ppm were also observed due to the $ArCH_2N$ and OCH_2N units of the oxazine ring. Also, the aromatic protons of the DDSQ-BZ (III) monomer remained the sharp

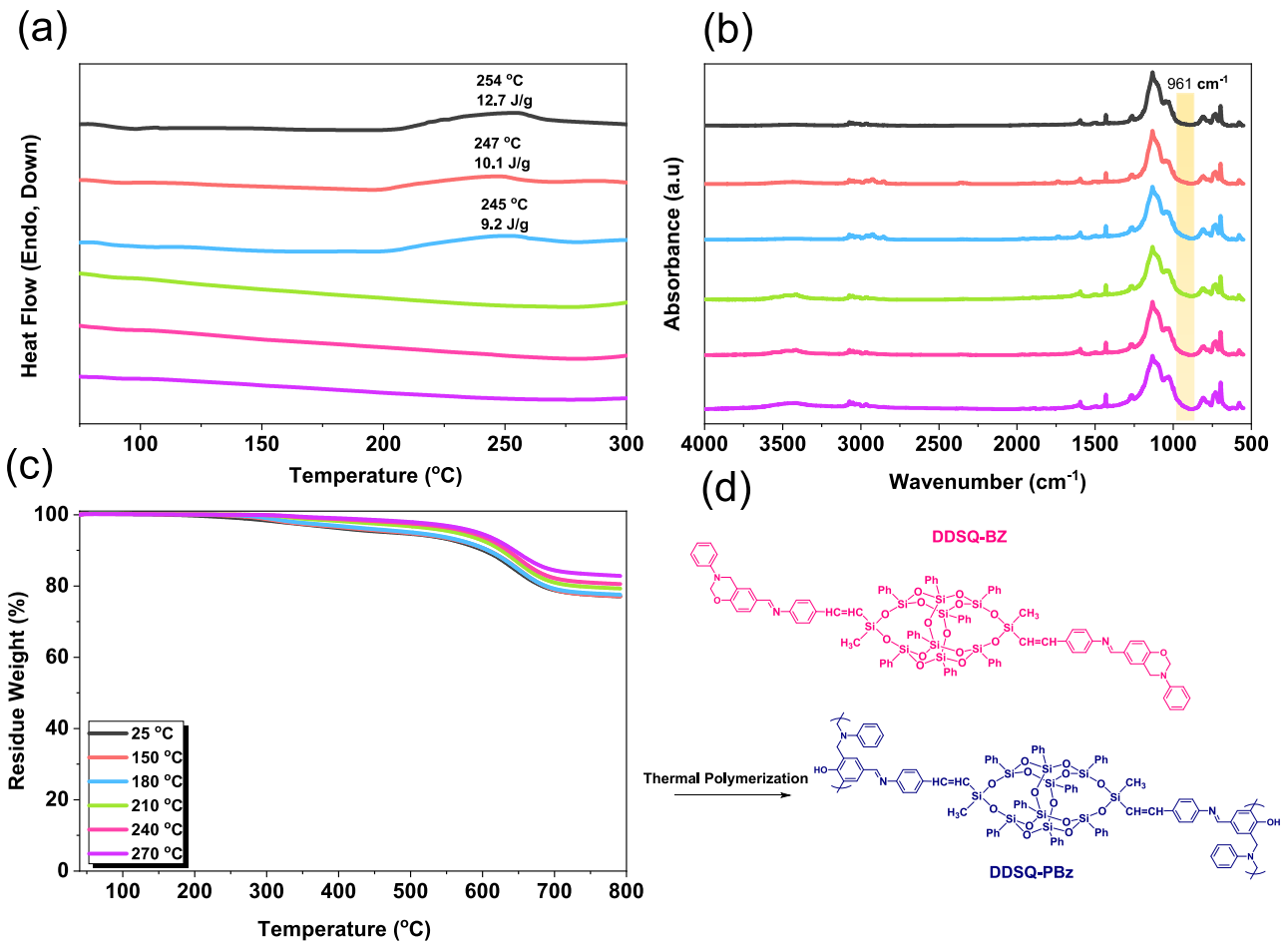

Fig. 7. (a) DSC, (b) FTIR, (c) TGA analyses of DDSQ-BZ (III) under thermal ROP at various temperatures, and (d) the possible thermal ROP behavior and the chemical structures change.

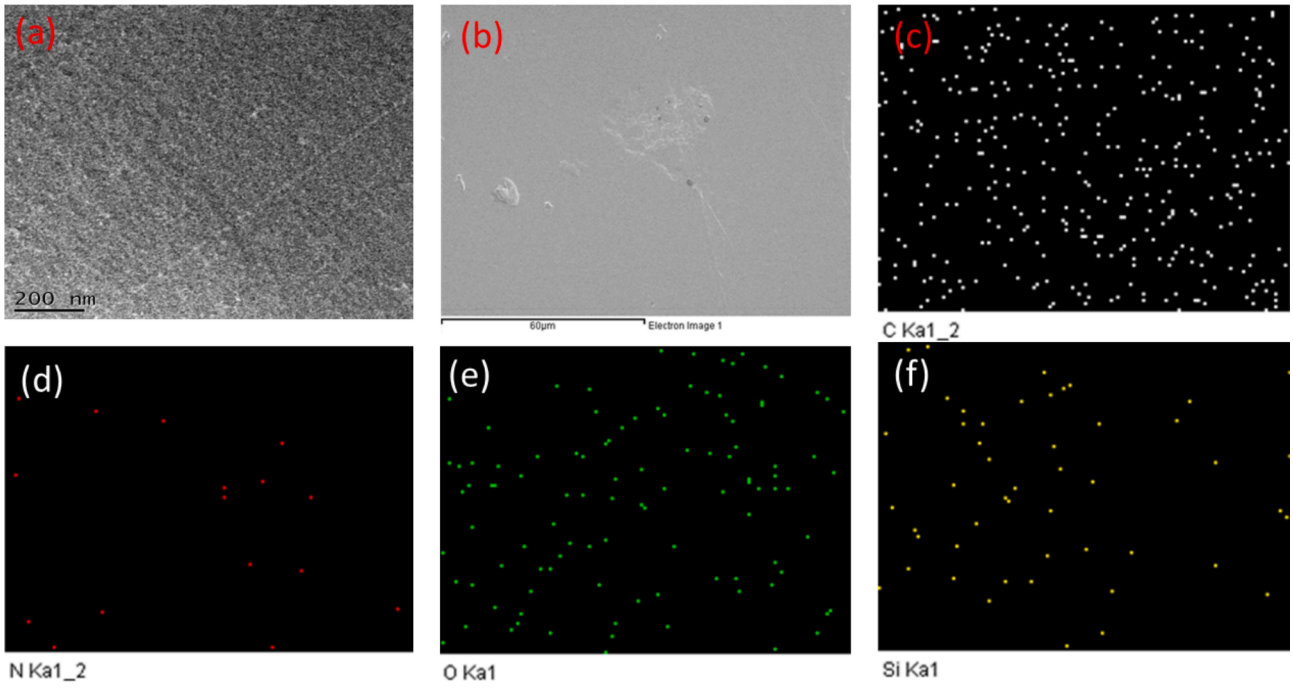

Fig. 8. (a) TEM, (b) SEM, (c-f) EDX analyses of (c) C-, (d) N-, (e) O-, and (f) Si-mapping of DDSQ-BZ (III) after thermal ROP.

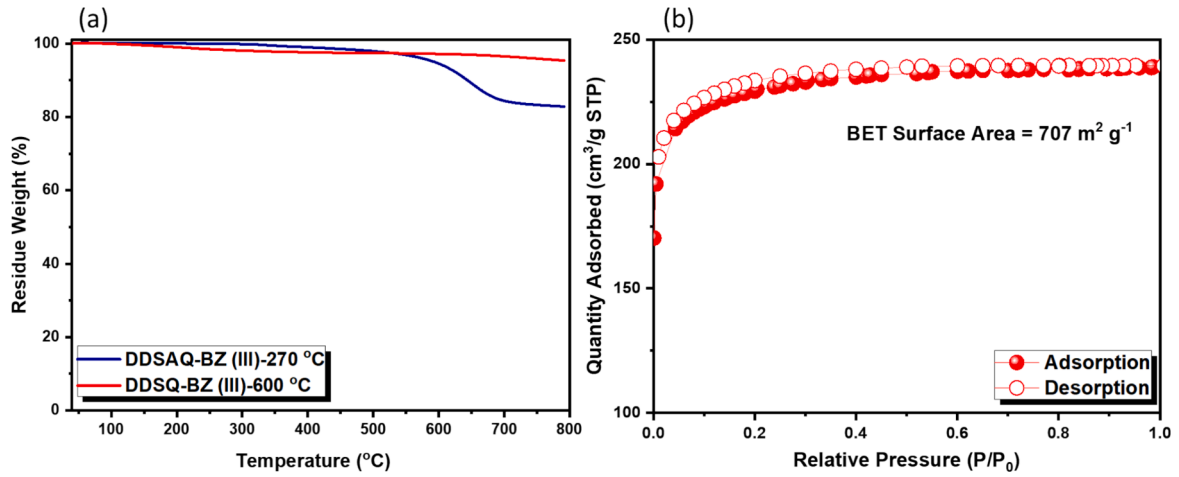

Fig. 9. (a) TGA analyses of DDSQ-BZ (III) after thermal ROP and carbonization at 600 °C and (b) N_2 adsorption/desorption isothermal analyses at 77 K.

peaks, suggesting the fully closed condensed cage DDSQ structure. These results collectively could confirm the successful construction of the DDSQ-BZ (III) monomer featuring the fully closed condensed cage DDSQ structure and oxazine ring simultaneously following the Schiff-base reaction in this study.

3.5. Thermal polymerization of DDSQ-BZ (III) monomer

Fig. 7**(a)** shows that DSC analyses of the DDSQ-BZ (III) showed the thermal ROP peak at 254 °C with the heat of enthalpy of 12.7 J g^{-1}. The thermal ROP peak becomes broad, and enthalpy is similar to CHO-BZ by considering the molecular weight of DDSQ-BZ (III) as expected. After thermal ROP of the DDSQ-BZ (III) monomer at 150 and 180 °C, with the thermal enthalpy of 10.1 and 9.2 J g^{-1}, respectively. The absence of oxazine ring in the DDSQ-BZ (III) was observed after thermal ROP at 210 °C for 2 h. Furthermore, Fig. 7**(b)** displayed FTIR data at diverse thermal ROP temperatures from 25 to 270 °C to investigate the thermal ROP of the DDSQ-BZ (III) monomer. The absorption intensity of the peak at 961 cm^{-1} was decreased upon increasing ROP temperature [**Fig. S3**] and disappeared at 210 °C, implying complete ROP. The remaining Si-O-Si unit at 1133 cm^{-1} after thermal ROP suggests the complete closed full cage structure of the DDSQ derivative. We also employed TGA thermal analyses to understand the thermal stability of the DDSQ-BZ (III) at distinct ROP temperatures as displayed in Fig. 7**(c)**. The pure DDSQ-BZ (III) monomer possesses very high heat resistance of T_{d5} value of 475 °C, T_{d10} value of 600 °C, and char yield of 77.1 wt%, which are significantly higher than CHO-BZ monomer because of rigid inorganic DDSQ cage structure [60,87,88]. The thermal degradation temperature (T_{d5}, T_{d10}) and char yield of the DDSQ-BZ (III) after ROP [270 °C] were significantly raised to 593 °C, 644 °C, and 82.8 wt%, respectively. As far as we know, thermal degradation temperatures and char yield are the highest values of benzoxazine monomer and polybenzoxazine resin. For example, the typical Pa-type PBZ with T_{d5} = 340 °C and the char yield is only 35 wt% [72–74] after thermal ROP even its thermal ROP peak at 263 °C. We also used the thermal aging test by the TGA analyses for pure CHO-BZ and DDSQ-BZ (III) monomers as shown in **Fig. S4**. The temperature was held at 250 °C for 1 day, the data were analyzed to understand the thermal stability of both benzoxazine monomers. The result indicates that the DDSQ-BZ (III) monomer displayed much higher char yield (97.88 wt%) and heat resistance as compared with pure CHO-BZ monomer after thermal ROP (96.08 wt%).

As a result, the incorporation of DDSQ into PBZ could enhance its thermal stability and char yield because of the silica-cage structure, which is usually highly thermal stable and resists decomposition at high temperatures and the possible chemical structure and mechanism was summarized in Fig. 7**(d)**. In addition, the rigid cage structure of DDSQ limits the mobility of the polymer chain and thus slows down thermal decomposition further, the DDSQ undergoes oxidation could form the silica-rich char, which could act as the protective barrier for the increase of char yield. Also, the vinyl double bond (C=C) and imine (C=N) bond could provide the extra cross-linking density that may also increase the heat resistance of DDSQ-BZ (III) after thermal ROP. The dispersion of the DDSQ cage structure in polybenzoxazine could be characterized by using TEM, SEM, and energy dispersive X-ray spectroscopy (EDX) analyses as shown in Fig. 8. Fig. 8**(a) and 8(b)** displayed the TEM and SEM images of the DDSQ-BZ (III) monomer after thermal ROP, revealing that the DDSQ cage structures are homogeneously dispersed and there is no discernible phase separation within the PBZ matrix [88–90]. Fig. 8**(c)-8 (f)** showed C, N, O, and Si-mapping of DDSQ-BZ (III) after thermal ROP and also suggested that the DDSQ cage was dispersed uniformly on the surface.

Since the DDSQ-BZ (III) monomer after thermal ROP has high thermal stability, it could form the microporous carbon/silica material with a high surface area and thus the DDSQ-BZ (III) monomer was placed in a tubular furnace at 600 °C under N_2 atmosphere. Fig. 9**(a)** shows the TGA analyses of poly(DDSQ-BZ) (III) and its corresponding microporous carbon/silica material. Clearly, the T_{d5} and char yield values significantly increased to higher than 800 °C and 95.8 wt%. As illustrated in Fig. 9**(b)**, the porosity characteristics of this microporous carbon/silica material were assessed using N_2 adsorption/desorption isothermal studies at 77 K. According to the IUPAC classification, the results showed type I isotherms. Since it had the sharp N_2 uptake at a relatively lower pressure (P/P_0), due to the presence of micropore characteristics resulting from the carbonization process [91] the framework exhibited S_{BET} surface area of 707 m^2 g^{-1}. We could expect that this microporous carbon/silica material may have some potential applications in energy storage, and gas capture or storage.

4. Conclusions

This study has prepared a new DDSQ-based benzoxazine monomer, focusing on its enhanced heat resistance and potential applications in high-performance materials. The integration of diamine-functionalized DDSQ cage structures into benzoxazine resin has demonstrated promising improvements over traditional benzoxazine formulations. One-pot Mannich condensation (DDSQ-BZ (I)) and three-step synthesis (DDSQ-BZ (II)) based on diamine DDSQ (DDSQ-NH_2) compound, were explored but proved unsuccessful due to low selectivity and DDSQ structural degradation. The DDSQ-BZ (III) was only successfully synthesized through a Schiff-base reaction between DDSQ-NH_2 and CHO-BZ, maintaining the fully closed-cage DDSQ structure and the formation of the benzoxazine ring. After thermal ROP, the DDSQ-BZ (III) exhibited

outstanding and record-high thermal stability, with T_{d5} = 593 °C, T_{d10} = 644 °C, and char yield of 82.8 wt% because of the homogeneous dispersion of inorganic DDSQ cage structure within the benzoxazine matrix, ensuring enhanced heat resistance. In addition, the formation of microporous carbon/silica material with a high surface area of 707 $m^2 g^{-1}$ after thermal treatment at 600 °C under N_2 atmosphere. In conclusion, this study contributes to the ongoing development of high-performance benzoxazine resins by demonstrating the feasibility and benefits of diamine-functionalized DDSQ incorporation, which are critical for applications in advanced composites, aerospace materials, and electronic packaging because of their potential in superior thermal, mechanical, and flame-resistant properties.

CRediT authorship contribution statement

Hui-Wen Chen: Methodology, Investigation, Formal analysis, Data curation, Conceptualization. **Mohamed Gamal Mohamed:** Writing – review & editing, Writing – original draft, Supervision, Data curation, Conceptualization. **Yang-Chin Kao:** Formal analysis, Data curation. **Wei-Cheng Chen:** Formal analysis. **Kevin Chiou:** Supervision. **Shiao-Wei Kuo:** Supervision, Resources, Project administration.

Declaration of competing interest

The authors declare that they have no known competing financial interests or personal relationships that could have appeared to influence the work reported in this paper.

Acknowledgements

This study was supported financially by the National Science and Technology Council, Taiwan, under contracts NSTC 112-2223-E-110-002- and 112-2218-E-110-007. The authors thank the staff at National Sun Yat-sen University (Taiwan) for their assistance with the TEM (ID: EM022600) experiments.

Appendix A. Supplementary data

Supplementary data to this article can be found online at https://doi.org/10.1016/j.eurpolymj.2025.113929.

Data availability

The data that has been used is confidential.

References

[1] J.W. Lim, Polymer Materials for Optoelectronics and Energy Applications, Materials 17 (2024) 3698, https://doi.org/10.3390/ma17153698.
[2] S. Jana, A. Parthiban, W. Rusli, Polymer material innovations for a green hydrogen economy, Chem. Commun. 61 (2025) 3233–3249, https://doi.org/10.1039/D4CC05750C.
[3] M.A. Shahid, M.M. Rahman, M.T. Hossain, I. Hossain, M.S. Sheikh, M.S. Rahman, N. Uddin, S.W. Donne, M.I.U. Hoque, Advances in Conductive Polymer-Based Flexible Electronics for Multifunctional Applications, J. Compos. Sci. 9 (2025) 42, https://doi.org/10.3390/jcs9010042.
[4] Y. Liu, L. Yuan, G. Liang, A. Gu, Developing thermally resistant and strong biobased resin from benzoxazine synthesized using green solvents, Eur. Polym. J. 173 (2022) 111320, https://doi.org/10.1016/j.eurpolymj.2022.111320.
[5] X.L. Sha, P. Fei, X. Wang, Y. Gao, Y. Zhu, Z. Liu, R. Lv, Large free volume biobased benzoxazine resin: Synthesis and characterization, dielectric properties, thermal and mechanical properties, Eur. Polym. J. 198 (2023) 112420, https://doi.org/10.1016/j.eurpolymj.2023.112420.
[6] Y. Liu, L. Yuan, G. Liang, A. Gu, Preparation of Thermally Resistant and Mechanically Strong Biomass Benzoxazine Resins via Green Strategy, ACS Sustain. Chem. Eng. 12 (2024) 1247–1254, https://doi.org/10.1021/acssuschemeng.3c06195.
[7] Y. Lu, J. Liu, W. Zhao, K. Zhang, Bio-benzoxazine structural design strategy toward highly thermally stable and intrinsically flame-retardant thermosets, Chem. Eng. J. 457 (2023) 141232, https://doi.org/10.1016/j.cej.2022.141232.
[8] M.G. Mohamed, C.J. Li, M.A.R. Khan, C.C. Liaw, K. Zhang, S.W. Kuo, Formaldehyde-Free Synthesis of Fully Bio-Based Multifunctional Bisbenzoxazine Resins from Natural Renewable Starting Materials, Macromolecules 55 (2022) 3106–3115, https://doi.org/10.1021/acs.macromol.2c00417.
[9] S. Mukherjee, N. Amarnath, B. Lochab, Oxazine Ring-Substituted 4th Generation Benzoxazine Monomers & Polymers: Stereoelectronic Effect of Phenyl Substituents on Thermal Properties, Macromolecules 54 (2021) 10001–10016, https://doi.org/10.1021/acs.macromol.1c01582.
[10] X. Shen, L. Cao, Y. Liu, J. Dai, X. Liu, J. Zhu, J., S. Du., How Does the Hydrogen Bonding Interaction Influence the Properties of Polybenzoxazine? An Experimental Study Combined with Computer Simulation, Macromolecules 51 (2018) 4782–4799, https://doi.org/10.1021/acs.macromol.8b00741.
[11] Z. Deliballi, B. Kiskan, Y. Yagci, Advanced Polymers from Simple Benzoxazines and Phenols by Ring-Opening Addition Reactions, Macromolecules 53 (2020) 2354–2361, https://doi.org/10.1021/acs.macromol.0c00225.
[12] K. Zhang, Y. Liu, H. Ishida, Polymerization of an AB-Type Benzoxazine Monomer toward Different Polybenzoxazine Networks: When Diels–Alder Reaction Meets Benzoxazine Chemistry in a Single-Component Resin, Macromolecules 52 (2019) 7386–7395, https://doi.org/10.1021/acs.macromol.9b01581.
[13] R. Yang, Z. Zhang, Design and Synthesis of Flavonoid-Based Mono-, Bis-, and Tri-Benzoxazines: Toward Elucidating Roles of Oxazine Ring Number and Hydrogen Bonding on Their Polymerization Mechanisms and Thermal Properties, Macromolecules 58 (2025) 616–626, https://doi.org/10.1021/acs.macromol.1c01582.
[14] X. Yuanm, L. Liu, Y. Wang, Q. Jiang, Y. Shi, G. Wang, Tyrosine-based branched polybenzoxazines with antibacterial and surface fouling released performances for marine antifouling coatings, Prog. Org. Coat. 200 (2025) 108978, https://doi.org/10.1016/j.porgcoat.2024.108978.
[15] K.I. Aly, M.G. Mohamed, O. Younis, M.H. Mahross, M. Abdel-Hakimm, M. M. Sayed, Salicylaldehyde azine-functionalized polybenzoxazine: Synthesis, characterization, and its nanocomposites as coatings for inhibiting the mild steel corrosion, Prog. Org. Coat. 138 (2020) 105385, https://doi.org/10.1016/j.porgcoat.2019.105385.
[16] C.F. Wang, S.F. Chiou, F.H. Ko, J.K. Chen, C.T. Chou, C.F. Huang, S.W. Kuo, F. C. Chang, Polybenzoxazine as a Mold-Release Agent for Nanoimprint Lithography, Langmuir 23 (2007) 5868–5871, https://doi.org/10.1021/la062921e.
[17] H.A. Klfout, A.M. Asiri, K.A. Alamry, M.A. Hussein, Recent advances in bio-based polybenzoxazines as an interesting adhesive coating, RSC Adv. 13 (2023) 19817–19835, https://doi.org/10.1039/D3RA03514J.
[18] S. Appasamy, B. Krishnasamy, S. Ramachandran, A. Muthukaruppan, Vanillin derived partially bio-based benzoxazine resins for hydrophobic coating and anticorrosion applications: Studies on syntheses and thermal behavior, Polym.-Plast. Technol. 63 (2024) 287–298, https://doi.org/10.1080/25740881.2023.2283772.
[19] M.G. Mohamed, S.W. Kuo, Functional Silica and Carbon Nanocomposites Based on Polybenzoxazines, Macromol. Chem. Phys. 220 (2019) 1800306, https://doi.org/10.1002/macp.201800306.
[20] M. Ejaz, M.G. Mohamed, W.C. Huang, Y.C. Kao, W.C. Chen, S.W. Kuo, Highly thermally stable polyhedral oligomeric silsesquioxane based on diacetal-functionalized polybenzoxazine nanocomposites, Eur. Polym. J. 223 (2025) 113649, https://doi.org/10.1016/j.eurpolymj.2024.113649.
[21] M.M. Samy, M.G. Mohamed, S.W. Kuo, Pyrene-functionalized tetraphenylethylene polybenzoxazine for dispersing single-walled carbon nanotubes and energy storage, Compos. Sci. Technol. 199 (2020) 108360, https://doi.org/10.1016/j.compscitech.2020.108360.
[22] X. Fan, S. Li, C. Wang, Y. Deng, C. Zhang, Z. Wang, Research on fluoropyridine-based benzoxazine with high thermal stability and excellent flame retardancy for its application in coatings, Eur. Polym. J. 187 (2023) 111884, https://doi.org/10.1016/j.eurpolymj.2023.111884.
[23] Y. Lyu, H. Ishida, Natural-sourced benzoxazine resins, homopolymers, blends and composites: A review of their synthesis, manufacturing and applications, Prog. Polym. Sci. 99 (2019) 101168, https://doi.org/10.1016/j.progpolymsci.2019.101168.
[24] E.A. Gorbunova, L.A. Soboleva, V.V. Shutov, M.V. Gorlov, V.V. Kireev, L.S. Sirotin, Structure-Property Relationship of Diaminodiphenylmethane-Based Benzoxazines–Precursors for High-Performance Thermoset Polymers, ACS Appl. Polym. Mater. 6 (2024) 11103–11109, https://doi.org/10.1021/acsapm.4c01318.
[25] M. Ejaz, M.G. Mohamed, S.W. Kuo, Solid state chemical transformation provides a fully benzoxazine-linked porous organic polymer displaying enhanced CO_2 capture and supercapacitor performance, Polym. Chem. 14 (2023) 2494–2509, https://doi.org/10.1039/D3PY00158J.
[26] X. Li, J. Huang, Y. Chen, F. Zhu, Y. Wang, W. Wei, Y. Feng, Polymer-Based Electronic Packaging Molding Compounds, Specifically Thermal Performance Improvement: An Overview, ACS Appl. Polym. Mater. 6 (2024) 14948–14969, https://doi.org/10.1021/acsapm.4c03086.
[27] B. Kiskan, Adapting benzoxazine chemistry for unconventional applications, React. Funct. Polym. 129 (2018) 76–88, https://doi.org/10.1016/j.reactfunctpolym.2017.06.009.
[28] M. Erdeger, B. Kiskan, F.S. Gungor, Synthesis and characterization of pyrrole-based benzoxazine monomers and polymers, Eur. Polym. J. 179 (2022) 111532, https://doi.org/10.1016/j.eurpolymj.2022.111532.
[29] M. Selvi, S. Devaraju, K. Sethuraman, M. Alagar, Carbon black–polybenzoxazine nanocomposites for high K dielectric applications, Polym. Compos. 35 (2014) 2121–2128, https://doi.org/10.1002/pc.22874.
[30] Q. Chen, R. Xu, D. Yu, Multiwalled carbon nanotube/polybenzoxazine nanocomposites: Preparation, characterization and properties, Polymer 47 (2006) 7711–7719, https://doi.org/10.1016/j.polymer.2006.08.058.

[31] M.G. Mohamed, K.C. Hsu, S.W. Kuo, Bifunctional polybenzoxazine nanocomposites containing photo-crosslinkable coumarin units and pyrene units capable of dispersing single-walled carbon nanotubes, Polym. Chem. 6 (2015) 2423–2433, https://doi.org/10.1039/C5PY00035A.
[32] C.R. Arza, H. Ishida, F.H. Maurer, Quantifying Dispersion in Graphene Oxide/Reactive Benzoxazine Monomer Nanocomposites, Macromolecules 47 (2014) 3685–3692, https://doi.org/10.1021/ma500334j.
[33] F. Meng, H. Ishida, X. Liu, Introduction of benzoxazine onto the graphene oxide surface by click chemistry and the properties of graphene oxide reinforced polybenzoxazine nanohybrids, RSC Adv. 4 (2014) 9471–9475, https://doi.org/10.1039/C3RA47345G.
[34] N. Kavitha, A. Chandramohan, K. Dinakaran, P. Prabukanthan, Recent developments in the polybenzoxazine based bionanocomposites: A review, Polym. Adv. Technol. 35 (2024) e6466.
[35] P.P. Jr, Y.L. Liu, B. Arnel, Effect of a direct sulfonation reaction on the functional properties of thermally-crosslinked electrospun polybenzoxazine (PBz) nanofibers, RSC Adv. 10 (2020) 14198, https://doi.org/10.1039/D0RA01285H.
[36] W. Wang, H. Liu, L. Pei, H. Liu, M. Wang, S. Li, Z. Wang, Modified polybenzoxazine and carbon fiber surface with improved mechanical properties by introducing hydrogen bonds, Eur. Polym. J. 182 (2023) 111717, https://doi.org/10.1016/j.eurpolymj.2022.111717.
[37] Q. Chen, R. Xu, J. Zhang, D. Yu, Polyhedral Oligomeric Silsesquioxane (POSS) Nanoscale Reinforcement of Thermosetting Resin from Benzoxazine and Bisoxazoline, Macromol. Rapid Commun. 26 (2005) 1878–1882, https://doi.org/10.1002/marc.200500511.
[38] I. Machado, E. Rachita, E. Fuller, V.M.A. Calado, H. Ishida, Very high-char-yielding elastomers based on the copolymers of a catechol/furfurylamine benzoxazine and polydimethylsiloxane oligomers, ACS Sustainable Chem. Eng. 9 (2021) 16637–16650, https://doi.org/10.1021/acssuschemeng.1c05408.
[39] R. Yang, L. Xie, N. Li, P. Froimowicz, K. Zhang, Synthesis of a triptycene-containing dioxazine benzoxazine monomer and a main-chain triptycene-polydimethysiloxane-benzoxazine copolymer with excellent comprehensive properties, Polym. Chem. 13 (2022) 3639–3649, https://doi.org/10.1039/D2PY00244B.
[40] R. Ganfoud, L. Puchot, T. Fouquet, P. Verge, H-bonding supramolecular interactions driving the dispersion of kaolin into benzoxazine: a tool for the reinforcement of polybenzoxazines thermal and thermo-mechanical properties, Compos. Sci. Technol. 110 (2015) 1–7, https://doi.org/10.1016/j.compscitech.2015.01.014.
[41] A.A. Alhwaige, H. Ishida, S. Qutubuddin, Chitosan/polybenzoxazine/clay mixed matrix composite aerogels: preparation, physical properties, and water absorbency, Appl. Clay Sci. 184 (2020) 105403, https://doi.org/10.1016/j.clay.2019.105403.
[42] K. Zhang, Q. Zhuang, X. Liu, G. Yang, R. Cai, Z. Han, A New Benzoxazine Containing Benzoxazole-Functionalized Polyhedral Oligomeric Silsesquioxane and the Corresponding Polybenzoxazine Nanocomposites, Macromolecules 46 (2013) 2696–2704, https://doi.org/10.1021/ma400243t.
[43] L. Miao, L.L. Zhan, S.L. Liao, Y. Li, T. He, S.C. Yin, L.B. Wu, H.Y. Qiu, The Recent Advances of Polymer-POSS Nanocomposites with Low Dielectric Constant, Macromol. Rapid Commun. 45 (2024) 2300601, https://doi.org/10.1002/marc.202300601.
[44] M.G. Mohamed, S.W. Kuo, Polybenzoxazine/Polyhedral Oligomeric Silsesquioxane (POSS) Nanocomposites, Polymers 8 (2016) 225–244, https://doi.org/10.3390/polym8060225.
[45] J. Faghihi, A.A. Azar, H.A. Khonakdar, M. Tohidian, Thermal stability and decomposition kinetics of polybenzoxazine and oligomeric polyhedral octaphenyl silsesquioxane nanocomposites, Polym. Adv. Technol. 35 (2024) e6459.
[46] Y. He, A. Suliga, A. Brinkmeyer, M. Schenk, I. Hamerton, Effect of atomic oxygen exposure on polybenzoxazine/POSS nanocomposites for space applications, Compos. Part a: Appl. Sci. Manuf. 177 (2024) 107898, https://doi.org/10.1016/j.compositesa.2023.107898.
[47] Y.K. Chang, S.J. Hao, F.G. Wu, Recent Biomedical Applications of Functional Materials Based on Polyhedral Oligomeric Silsesquioxane (POSS), Small 20 (2024) 2401762, https://doi.org/10.1002/smll.202401762.
[48] W.W. Young, J.P. Saez, R. Katsumata, Rationalizing the Composition Dependence of Glass Transition Temperatures in Amorphous Polymer/POSS Composites, ACS Macro Lett. 10 (2021) 1404–1409, https://doi.org/10.1021/acsmacrolett.1c00597.
[49] K.N. Raftopoulos, K. Pielichowski, Segmental dynamics in hybrid polymer/POSS nanomaterials, Prog. Polym. Sci. 52 (2016) 136–187, https://doi.org/10.1016/j.progpolymsci.2015.01.003.
[50] X. Ye, X. Jing, Y. Liu, Z. Han, F. Yang, L. Qiao, J. Ren, L. Meng, Z. Li, W. Wang, J. Li, Y. Li, Simultaneously Flame Retarding and Toughening of Epoxy Resin Composites Based on Two-Dimensional Polyhedral Oligomeric Silsesquioxane/Polyoxometalate Supramolecular Nanocrystals with Ultralow Loading, ACS Appl. Mater. Interfaces 16 (2024) 49763–49777, https://doi.org/10.1021/acsami.4c09639.
[51] M.G. Mohamed, M.H. Elsayed, A.E. Hassan, A. Basit, I.M.A. Mekhemer, H.H. Chou, K.H. Chen, S.W. Kuo, Hybrid Porous Polymers Combination of Octavinylsilsesquioxane/Pyrene with Benzothiadiazole Units for Robust Energy Storage and Efficient Photocatalytic Hydrogen Production from Water, ACS Appl. Polym. Mater. 6 (2024) 5945–5956, https://doi.org/10.1021/acsapm.4c00655.
[52] C.W. Hsiao, A.M. Elewa, M.G. Mohamed, S.W. Kuo, Highly stable hybrid porous polymers containing polyhedral oligomeric silsesquioxane (POSS)/Dibenzo[g,p]chrysene and Dibenzo[b,d]thiophene units for efficient Rhodamine B dye removal, Sep. Purif. Technol. 332 (2024) 125771, https://doi.org/10.1016/j.seppur.2023.125771.
[53] S.W. Kuo, F.C. Chang, POSS related polymer nanocomposites, Prog. Polym. Sci. 36 (2011) 1649–1696, https://doi.org/10.1016/j.progpolymsci.2011.05.002.
[54] M.G. Mohamed, S.W. Kuo, Progress in the self-assembly of organic/inorganic polyhedral oligomeric silsesquioxane (POSS) hybrids, Soft Matter 18 (2022) 5535–5561, https://doi.org/10.1039/D2SM00635A.
[55] S.W. Kuo, Hydrogen bonding interactions in polymer/polyhedral oligomeric silsesquioxane nanomaterials, J. Polym. Res. 29 (2022) 69, https://doi.org/10.1007/s10965-021-02885-4.
[56] Y.J. Lee, S.W. Kuo, Y.C. Su, J.K. Chen, C.W. Tu, F.C. Chang, Syntheses, thermal properties, and phase morphologies of novel benzoxazines functionalized with polyhedral oligomeric silsesquioxane (POSS) nanocomposites, Polymer 45 (2004) 6321–6331, https://doi.org/10.1016/j.polymer.2004.04.055.
[57] Y.C. Wu, S.W. Kuo, Synthesis and Characterization of Polyhedral Oligomeric Silsesquioxane (POSS) with Multifunctional Benzoxazine Groups Through Click Chemistry, Polymer 51 (2010) 3948–3955, https://doi.org/10.1016/j.polymer.2010.06.033.
[58] W.H. Hu, K.W. Huang, C.W. Chiou, S.W. Kuo, Complementary Multiple Hydrogen Bonding Interactions Induce the Self-Assembly of Supramolecular Structures from Heteronucleobase-Functionalized Benzoxazine and Polyhedral Oligomeric Silsesquioxane Nanoparticles, Macromolecules 45 (2012) 9020–9028, https://doi.org/10.1021/ma302077x.
[59] X. Sun, J. Wang, Q. Fu, Q. Zhang, R. Xu, Synthesis of a Novel Bifunctional Epoxy Double-Decker Silsesquioxane: Improvement of the Thermal Stability and Dielectric Properties of Polybenzoxazine, Polymers 14 (2022) 5154, https://doi.org/10.3390/polym14235154.
[60] C.H. Lin, W.B. Chen, W.T. Whang, C.H. Chen, Characteristics of Thermosetting Polymer Nanocomposites: Siloxane-Imide-Containing Benzoxazine with Silsesquioxane Epoxy Resins, Polymers 12 (2020) 2510, https://doi.org/10.3390/polym12112510.
[61] N. Liu, L. Li, L. Wang, S. Zheng, Organic-inorganic polybenzoxazine copolymers with double decker silsesquioxanes in the main chains: Synthesis and thermally activated ring-opening polymerization behavior, Polymer 109 (2017) 254–265, https://doi.org/10.1016/j.polymer.2016.12.049.
[62] M. Wang, H. Chi, J.K. S, F. Wang. Progress in the Synthesis of Bifunctionalized Polyhedral Oligomeric Silsesquioxane. Polymers 11 (2019) 2098. Doi: 10.3390/polym11122098.
[63] S. Wu, T. Hayakawa, M.A. Kakimoto, H. Oikawa, Synthesis and Characterization of Organosoluble Aromatic Polyimides Containing POSS in Main Chain Derived from Double-Decker-Shaped Silsesquioxane, Macromolecules 41 (2008) 3481–3487, https://doi.org/10.1021/ma7027227.
[64] S. Wu, T. Hayakawa, R. Kikuchi, S.J. Grunzinger, M.A. Kakimoto, H. Oikawa, Synthesis and Characterization of Semiaromatic Polyimides Containing POSS in Main Chain Derived from Double-Decker-Shaped Silsesquioxane, Macromolecules 40 (2007) 5698–5705, https://doi.org/10.1021/ma070547z.
[65] N. Liu, K. Wei, L. Wang, S. Zheng, Organic-inorganic polyimides with double decker silsesquioxane in the main chains, Polym. Chem. 7 (2016) 1158–1167, https://doi.org/10.1039/C5PY01827G.
[66] K. Wei, L. Wang, S. Zheng, Organic-inorganic polyurethanes with 3,13-dihydroxypropyloctaphenyl double-decker silsesquioxane chain extender, Polym. Chem. 4 (2013) 1491–1501, https://doi.org/10.1039/C2PY20930F.
[67] K. Wei, L. Wang, S. Zheng, Organic-inorganic copolymers with double-decker silsesquioxane in the main chains by polymerization via click chemistry. J. Polym. Sci. Part A, Polym. Chem. 51 (2013) 4221–4232, https://doi.org/10.1002/pola.26836.
[68] S. Xu, B. Zhao, K. Wei, S. Zheng, Organic–inorganic polyurethanes with double decker silsesquioxanes in the main chains: Morphologies, surface hydrophobicity, and shape memory properties, J. Polym. Sci. Part b. 56 (2018) 893–906, https://doi.org/10.1002/polb.24603.
[69] W.C. Chen, Y.H. Tsao, C.F. Wang, C.F. Huang, L. Dai, T. Chen, S.W. Kuo, Main Chain–Type Block Copolymers through Atom Transfer Radical Polymerization from Double-Decker–Shaped Polyhedral Oligomeric Silsesquioxane Hybrids, Polymers 12 (2020) 465, https://doi.org/10.3390/polym12020465.
[70] P. Groch, K. Dziubek, K. Czaja, M. Białek, K. Mituła, B. Dudziec, B. Marciniec, Synthesis and structural characterization of ethylene copolymers containing double-decker silsesquioxane as pendant groups and cross-linkage sites by coordinative copolymerization, Eur. Polym. J. 100 (2018) 187–199, https://doi.org/10.1016/j.eurpolymj.2018.01.039.
[71] P. Żak, B. Dudziec, M. Dutkiewicz, M. Ludwiczak, B. Marciniec, M. Nowicki, A new class of stereoregular vinylene-arylene copolymers with double-decker silsesquioxane in the main chain, J. Polym. Sci., Part a: Polym. Chem. 54 (2016) 1044–1055, https://doi.org/10.1002/pola.27957.
[72] Y.T. Liao, Y.C. Lin, S.W. Kuo, Highly Thermally Stable, Transparent, and Flexible Polybenzoxazine Nanocomposites by Combination of Double-Decker-Shaped Polyhedral Silsesquioxanes and Polydimethylsiloxane, Macromolecules 50 (2017) 5739–5747, https://doi.org/10.1021/acs.macromol.7b01085.
[73] W.C. Chen, S.W. Kuo, Ortho-Imide and Allyl Groups Effect on Highly Thermally Stable Polybenzoxazine/Double-Decker-Shaped Polyhedral Silsesquioxane Hybrids, Macromolecules 51 (2018) 9602–9612, https://doi.org/10.1021/acs.macromol.8b02207.
[74] C.Y. Chen, W.C. Chen, M.G. Mohamed, Z.Y. Chen, S.W. Kuo, Highly Thermally Stable, Reversible, and Flexible Main Chain Type Benzoxazine Hybrid Incorporating Both Polydimethylsiloxane and Double-Decker Shaped Polyhedral Silsesquioxane Units through Diels–Alder Reaction, Macromol. Rapid Commun. 44 (2023) 2200910, https://doi.org/10.1002/marc.202200910.
[75] Y.C. Kao, J.Y. Lin, W.C. Chen, M.G. Mohamed, C.F. Huang, J.H. Chen, S.W. Kuo, High-Thermal Stable Epoxy Resin through Blending Nanoarchitectonics with

Double-Decker-Shaped Polyhedral Silsesquioxane-Functionalized Benzoxazine Derivatives, Polymers 16 (2024) 112, https://doi.org/10.3390/polym16010112.
[76] A.M.M. Soliman, K.I. Aly, M.G. Mohamed, A.A. Amer, M.R. Belal, M. Abdel-Hakim, Synthesis, characterization and protective efficiency of novel polybenzoxazine precursor as an anticorrosive coating for mild steel, Sci. Rep. 13 (2023) 5581, https://doi.org/10.1038/s41598-023-30364-x.
[77] C.H. Lin, S.L. Chang, C.W. Hsieh, H.H. Lee, Aromatic diamine-based benzoxazines and their high-performance thermosets, Polymer 49 (2008) 1220–1229, https://doi.org/10.1016/j.polymer.2007.12.042.
[78] S. Ohashi, F. Cassidy, S. Huang, K. Chiou, H. Ishida, Synthesis and ring-opening polymerization of 2-substituted 1,3-benzoxazine: the first observation of the polymerization of oxazine ring-substituted benzoxazines, Polym. Chem. 7 (2016) 7177–7184, https://doi.org/10.1039/C6PY01686C.
[79] M.G. Mohamed, T.C. Chen, S.W. Kuo, Solid-State Chemical Transformations to Enhance Gas Capture in Benzoxazine-Linked Conjugated Microporous Polymers, Macromolecules 54 (2021) 5866–5877, https://doi.org/10.1021/acs.macromol.1c00736.
[80] M.G. Mohamed, W.C. Chang, S.W. Kuo, Crown Ether- and Benzoxazine-Linked Porous Organic Polymers Displaying Enhanced Metal Ion and CO_2 Capture through Solid State Chemical Transformation, Macromolecules 55 (2022) 7879–7892, https://doi.org/10.1021/acs.macromol.2c01216.
[81] M.G. Mohamed, C.C. Chen, K. Zhang, S.W. Kuo, Construction of three-dimensional porous organic polymers with enhanced CO_2 uptake performance via solid-state thermal conversion from tetrahedral benzoxazine-linked precursor, Eur. Polym. J. 200 (2023) 112551, https://doi.org/10.1016/j.eurpolymj.2023.112551.
[82] M.G. Mohamed, B.X. Su, S.W. Kuo, Robust Nitrogen-Doped Microporous Carbon via Crown Ether-Functionalized Benzoxazine-Linked Porous Organic Polymers for Enhanced CO_2 Adsorption and Supercapacitor Applications, ACS Appl. Mater. Interfaces 16 (2024) 40858, https://doi.org/10.1021/acsami.4c05645.
[83] M.G. Kotp, M.G. Mohamed, A.O. Mousa, S.W. Kuo, Rational design and molecular engineering of ultrastable porous fluorescent guanidine functionalized polybenzoxazine, Eur. Polym. J. 227 (2025) 113786, https://doi.org/10.1016/j.eurpolymj.2025.113786.
[84] K. Kuciński, H.S. Dłużyńska, G. Hreczycho, Catalytic silylation of O-nucleophiles via Si-H or Si-C bond cleavage: A route to silyl ethers, silanols and siloxanes, Coord. Chem. Rev. 459 (2022) 214456, https://doi.org/10.1016/j.ccr.2022.214456.
[85] H.M. Ma, Y. Liu, Y.X. Liu, J.J. Qiu, C.M. Liu, Vinyl benzoxazine: a novel heterobifunctional monomer that can undergo both free radical polymerization and cationic ring-opening polymerization, RSC Adv. 5 (2015) 102441–102447, https://doi.org/10.1039/C5RA18058A.
[86] X. Zhang, J. Hou, M. Wu, J. Ye, S. Zhang, X. Liu, Melamine as cross-linking agent for mono-cyclic benzoxazine with aldehyde groups: higher crosslinking density and thermal properties, J. Polym. Sci. 141 (2024) e54785, https://doi.org/10.1002/app.54785.
[87] Y. Xiao, X. Lei, Y. Liu, Y. Zhang, X. Ma, Q. Zhang, Double-decker-shaped phenyl-substituted silsesquioxane (DDSQ)-based nanocomposite polyimide membranes with tunable gas permeability and good aging resistance, Sep. Purif. Technol. 315 (2023) 123725, https://doi.org/10.1016/j.seppur.2023.123725.
[88] W.C. Chen, M.M.M. Ahmed, C.F. Wang, C.F. Huang, S.W. Kuo, Highly thermally stable mesoporous Poly(cyanate ester) featuring a double–decker–shaped polyhedral silsesquioxane framework, Polymer 185 (2019) 121940, https://doi.org/10.1016/j.polymer.2019.121940.
[89] S. Muhammad, J.H. Niazi, S. Shawuti, A. Anjum Qureshi, Functional POSS based polyimide nanocomposite for enhanced structural, thermal, antifouling and antibacterial properties, Mater. Today Commun. 31 (2022) 103287, https://doi.org/10.1016/j.mtcomm.2022.103287.
[90] Y.C. Kao, Y.H. Ku, M.G. Mohamed, W.H. Su, S.W. Kuo, Microphase Separation Transformation in Bio-Based Benzoxazine/Phenolic/PEO-b-PCL Diblock Copolymer Mixtures Induced by Transesterification Reaction, Macromolecules 58 (2025) 585–600, https://doi.org/10.1021/acs.macromol.4c02072.
[91] M. Ejaz, M.G. Mohamed, Y.T. Chen, K. Zhang, S.W. Kuo, Porous carbon materials augmented with heteroatoms derived from hyperbranched biobased benzoxazine resins for enhanced CO_2 adsorption and exceptional supercapacitor performance, J. Energy Storage 78 (2024) 110166, https://doi.org/10.1016/j.est.2023.110166.